



SUPPORTING INFORMATION

Thermoreversible luminescent ionogels with white light emission: An experimental and theoretical approach

Talita Jordanna de Souza Ramos,^a Rodrigo da Silva Viana,^a Leonardo Schaidhauer,^b Tania Cassol,^c Severino Alves Junior^a

^a Departamento de Química Fundamental, Universidade Federal de Pernambuco, Recife – PE, 50740-560, Brazil.

^b Escola de Alimentos, Universidade Federal do Rio Grande, Rio Grande – PR, 96.201-900, Brazil.

^c Universidade Tecnológica Federal do Paraná, São Francisco Beltrão – PR, 85601-970, Brazil.

Summary

| | |
|---|----|
| Fig. S1 Scheme for representation the synthesis route of ionic liquid and luminescent materials; Photographs acquired under daylight illumination and uv exposure | 2 |
| Fig S2: Structure for ionic liquid 3-(3-methyl-1H-imidazol-3-ium-1-yl) propane-1-sulfonate (IL) | 3 |
| Fig. S3 Nuclear magnetic resonance spectrum for ionic liquid (¹ H) | 3 |
| Fig. S4 Nuclear magnetic resonance spectrum for ionic liquid (¹³ C) | 4 |
| Fig. S5 Nuclear magnetic resonance spectrum for Eu-IL (¹ H) | 5 |
| Fig. S6 Nuclear magnetic resonance spectrum for Tb-IL (¹ H) | 5 |
| Fig. S7 Nuclear magnetic resonance spectrum for Gd-IL (¹ H) | 6 |
| Fig. S8: Thermalgravimetric analysis for IL, Eu-IL, Tb-IL and Gd-IL compounds | 7 |
| Fig. S9 Excitation spectrum for IL ligand ($\lambda_{EM} = 450$ nm) with temperature variation | 7 |
| Fig. S10 Emission spectrum for IL ligand ($\lambda_{EX} = 369$ nm) with temperature variation | 8 |
| Fig. S11 Excitation spectrum for Gd-IL ($\lambda_{EM} = 425$ nm) with temperature variation | 8 |
| Fig. S12 Emission spectrum for Gd-IL ($\lambda_{EM} = 350$ nm) with temperature variation | 9 |
| Fig. S13 Excitation spectrum for Eu-IL ($\lambda_{EM} = 616$ nm) with temperature variation | 9 |
| Fig. S14 Emission spectrum for Eu-IL ($\lambda_{EXC} = 395$ nm) with temperature variation | 10 |
| Fig. S15 ⁵ D ₁ → ⁷ F ₂ transitions in the emission spectrum for Eu-IL ($\lambda_{EXC} = 395$ nm) with temperature variation | 10 |
| Fig. S16 Exponential decay curves for the Eu-IL in function of temperature variation | 11 |
| Fig. S17 Excitation spectrum for Tb-IL ($\lambda_{EM} = 542$ nm) with temperature variation | 12 |
| Fig. S18 Emission spectrum for Tb-IL ($\lambda_{EXC} = 370$ nm) with temperature variation | 12 |
| Fig. S19 Exponential decay curves for the Tb-IL in function of temperature variation | 13 |
| Fig.S20 Reversibility experiment for the excitation spectrum of Eu-IL. system at room temperature (black), under heating to 100 °C (red) and after 24 hours in contact with moisture (gray) | 14 |
| Fig. S21 Reversibility experiment for the emission spectrum of Eu-IL. System at room temperature (black), under heating to 100 °C (red) and after 24 hours in contact with moisture (gray) | 15 |
| Fig.S22 Reversibility experiment for exponential decay curves of Eu-IL. System at room temperature (black), under heating to 100 °C (red) and after 24 hours in contact with moisture (gray) | 15 |
| Fig.S23 Reversibility experiment for the excitation spectrum of Tb-IL. System at room temperature (black line), under heating to 100 °C (green) and after 24 hours in contact with moisture (gray) | 16 |
| Fig.S24 Reversibility experiment for the emission spectrum of Tb-IL. System at room temperature (black), under heating to 100 °C (green) and after 24 hours in contact with moisture (gray) | 16 |

- Fig.S25** Reversibility experiment for exponential decay curves of Tb-IL. System at room temperature (black), under heating to 100 °C (green) and after 24 hours in contact with moisture (gray) 17
- Fig. S26** Coordination environment formed by ionic liquids and metal center of europium 17
- Fig. S27:** Energy level diagram for Eu-IL complex, showing the most probable channel for intramolecular energy transfer 18
- Fig. S28** Comparison of excitation spectrum for Eu-IL ($\lambda_{EM} = 616$ nm) obtained for the solution and rt conditions 18
- Fig. S29** Comparison of emission spectrum for Eu-IL ($\lambda_{EXC} = 395$ nm) obtained for the solution and RT conditions 19
- Fig. S30** Lifetime obtained for Eu-IL in solution ($\lambda_{EXC} = 395$ nm and $\lambda_{EM} = 616$ nm) 19
- Fig. S31.** Excitation spectrum of the mixed system TB_{25%}Eu_{25%}Gd_{50%}-IL monitored at 616 nm (red line) compared with the spectrum of Tb-IL compound monitored at 543 nm (green line) 20
- Fig. S32** Infrared spectrum for ionic liquid (IL) and mixed system (TB_{25%}Eu_{25%}Gd_{50%}-IL) 20
- Fig. S33** Thermalgravimetric analysis to mixed system (TB_{25%}Eu_{25%}Gd_{50%}-IL) 20

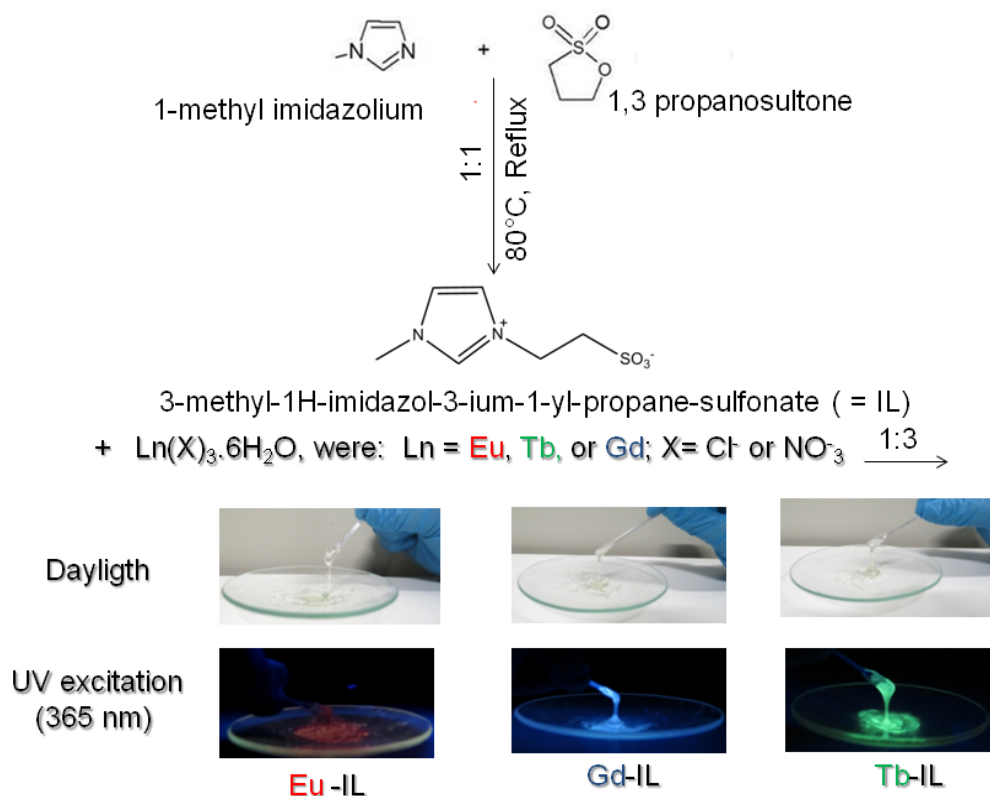


Fig. S1 Scheme for representation the synthesis route of ionic liquid and luminescent materials; photographs acquired under daylight illumination and UV exposure.

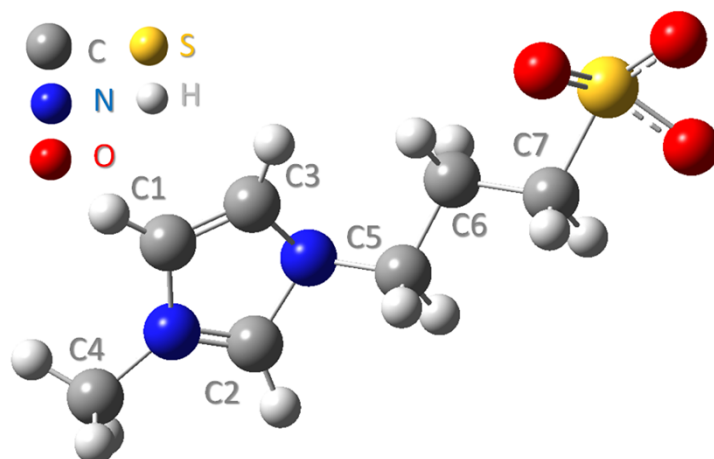


Fig. S2: Structure for ionic liquid 3-(3-methyl-1H-imidazol-3-ium-1-yl) propane-1-sulfonate (IL).

NMR interpretation for ionic liquid (dissolved in D_2O): 1H : δ = 1.9 ppm (m, 2H; C7); 2.2 ppm (t, 3H; C5); 3.2 ppm (s, residual water); 3.5 ppm (s, 3H; C4); 4.1 ppm (m, 4H; C6); 7.5 ppm (s, 1H; C2;C3); 8.9 ppm (s, 1H;C1). Spectrum is shown in S3. ^{13}C δ = 24.5ppm (C5); 27.1 ppm (C7); 47.9 ppm (C4); 68.7 ppm (C6); 119.5 ppm (C2; C3); 136,2 ppm (C1). These offsets were compared with other studies reported in the literature^{[1],[2]} for the synthesis of 3-(3-methyl-1H-imidazol-3-ium-1-yl) propane-1-sulfonate and certify the purity and structure of the material obtained. Spectrum for NMR to ^{13}C is shown in S4.

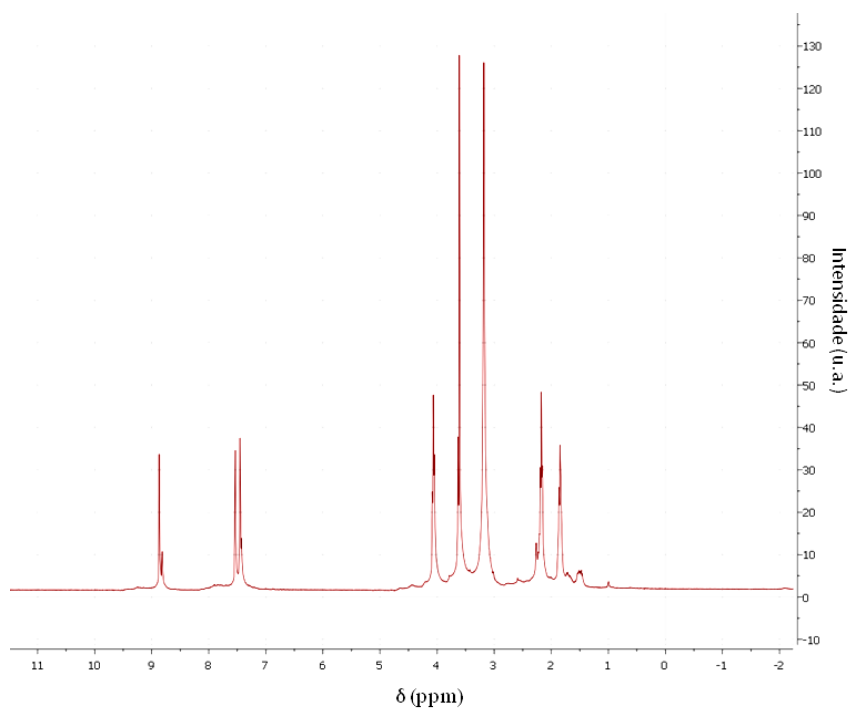


Fig. S3 Nuclear magnetic resonance spectrum for ionic liquid (1H).

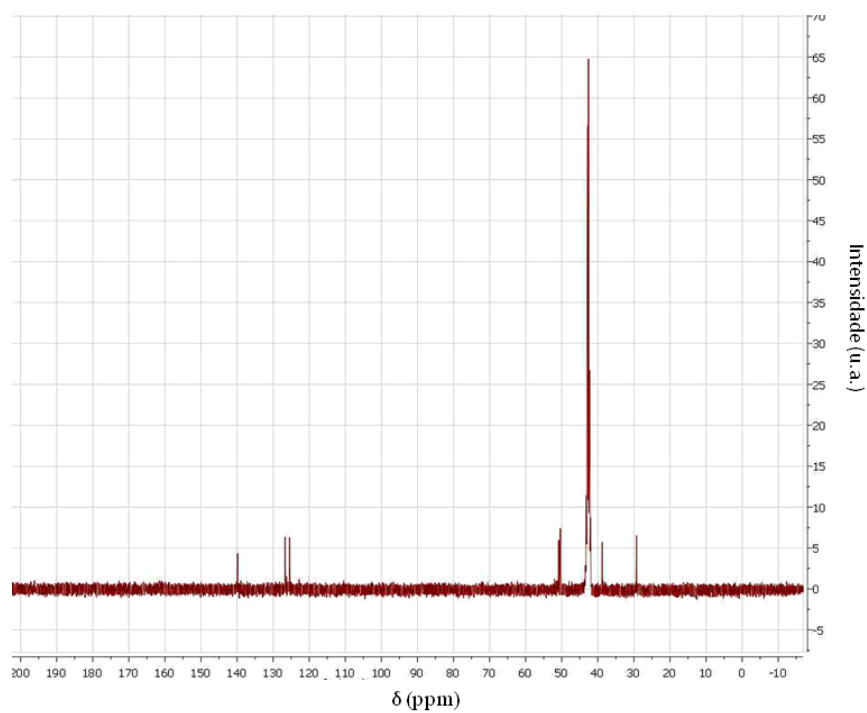


Fig. S4 Nuclear magnetic resonance spectrum for ionic liquid (^{13}C).

NMR ^1H interpretation for complex Eu-IL (dissolved in DMSO deuterated): $\Delta = 1.2$ ppm (m, 2H; C5); 1.6 ppm (m, 2H; C6); 2.15 ppm (m, 2H; C7), 3.0 ppm (s, residual water); 3.5 ppm (s, 3H; C4); 7.4 ppm (s, 1H; C4); 7.3 ppm (s, 1H; C3) 8.71 ppm (s, 1H; C1). These chemical shifts are consistent with maintaining the proposed structure of the ionic liquid (S2) after obtaining the luminescent materials. Spectrum is displayed in S5.

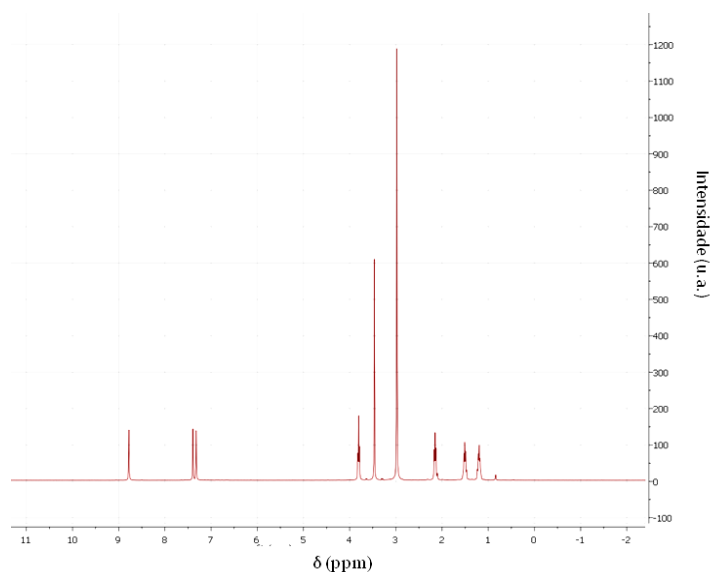


Fig. S5 Nuclear magnetic resonance spectrum for Eu-IL (^1H).

NMR ^1H interpretation for complex Tb-IL (dissolved in DMSO deuterated): $\Delta = 1.5$ ppm (1,0, 2H; C5); 2.0 ppm (m, 2H; C6); 2.5 ppm (m, 2H; C7); 3.70 ppm (residual water); 4.4 ppm (s, 3H; C4); 8.1 ppm (s, 2H; C2; C3); 9.6 ppm (s, 1H; C1). Spectrum is shown in S6.

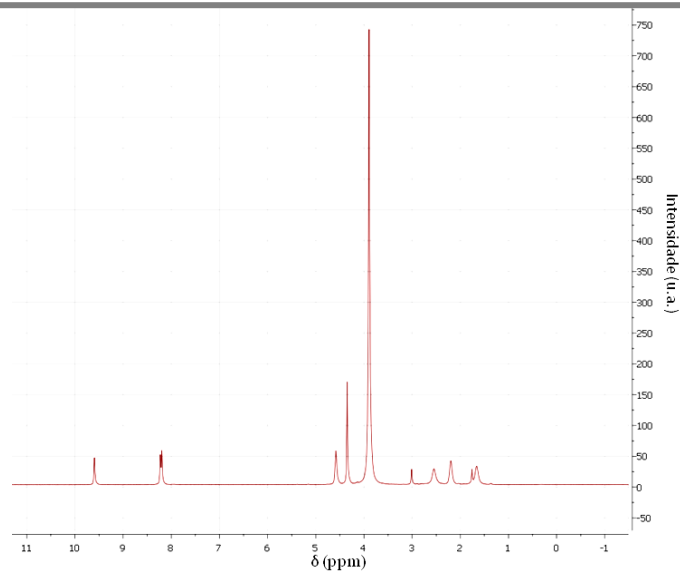


Fig. S6 Nuclear magnetic resonance spectrum for Tb-IL (^1H).

NMR ^1H interpretation for complex Li-Gd (dissolved in DMSO deuterated): difficult to interpret due to the paramagnetic effects of atom of Gd, are observed expanded lines, identifying the peaks of the aromatic H of the imidazolium cation. $\Delta = 8.5$ (s wide, 2H), 9.7 (s wide 1H; C1). Spectrum is submitted in S7.

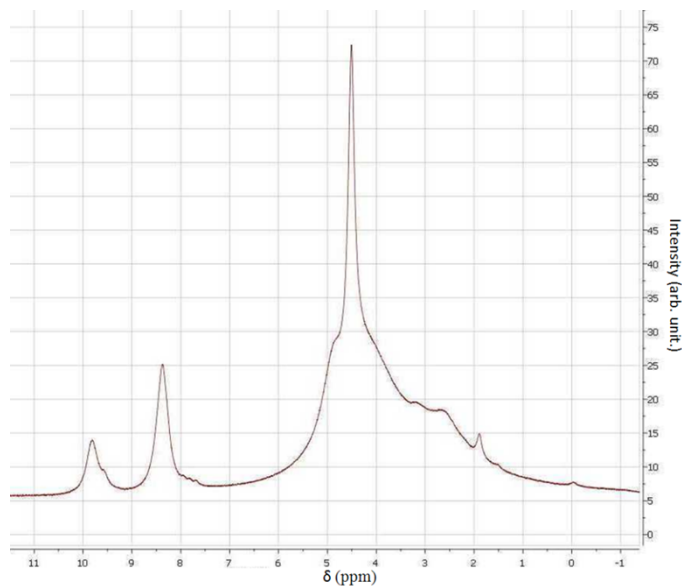


Fig. S7 Nuclear magnetic resonance spectrum for Gd-IL (^1H).

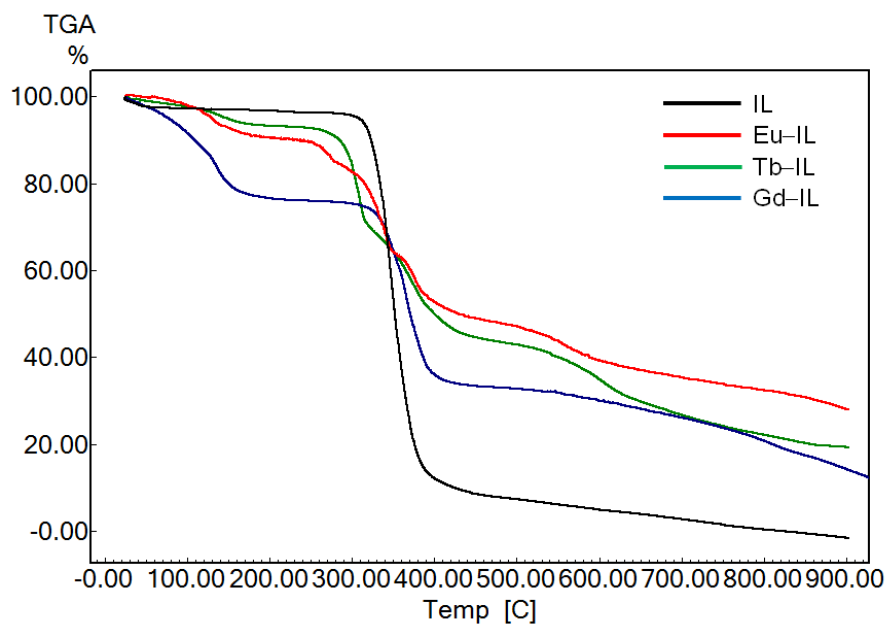


Fig. S8: Thermalgravimetric analysis for IL, Eu-IL, Tb-IL and Gd-IL compounds.

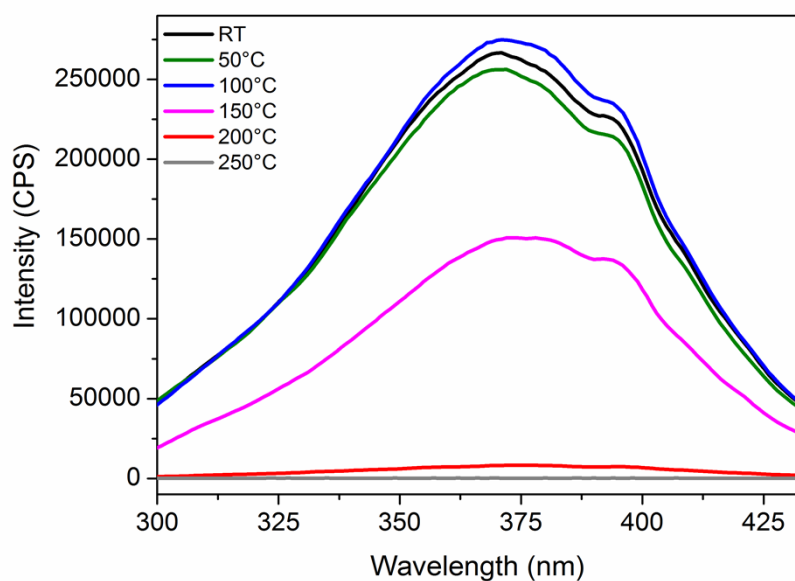


Fig. S9 Excitation spectrum for IL ligand ($\lambda_{em} = 450$ nm) with temperature variation.

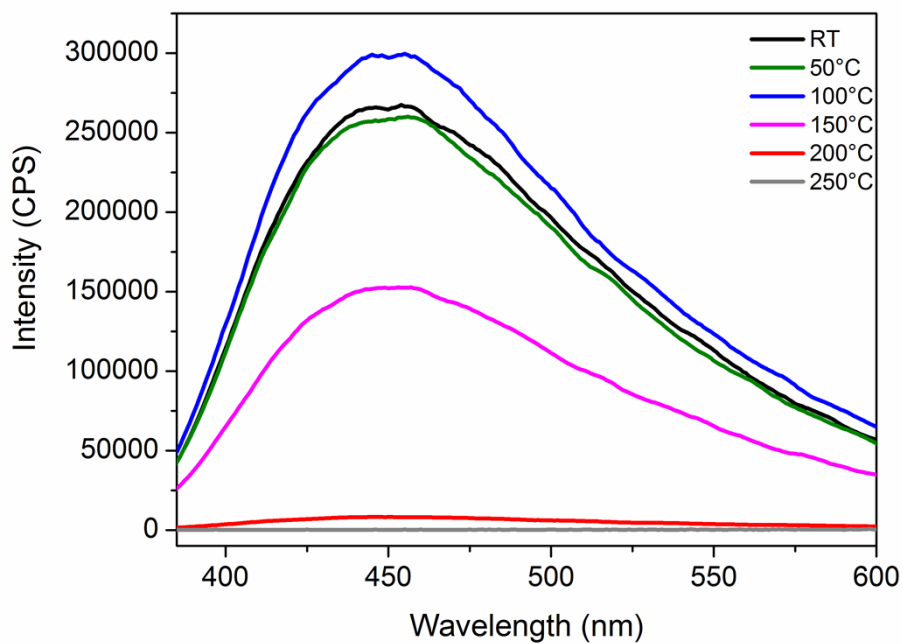


Fig. S10 Emission spectrum for IL ligand ($\lambda_{\text{ex}} = 369 \text{ nm}$) with temperature variation.

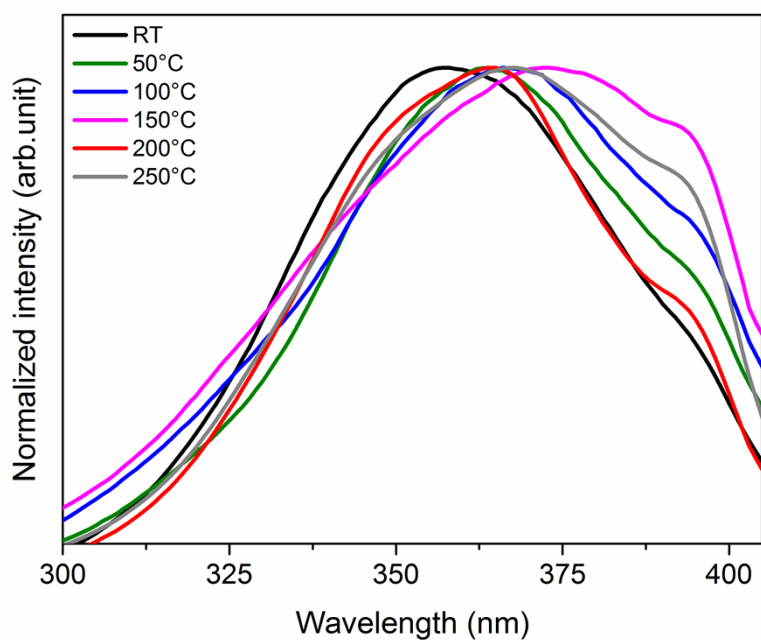


Fig. S11 Excitation spectrum for Gd-IL ($\lambda_{\text{em}} = 425 \text{ nm}$) with temperature variation.

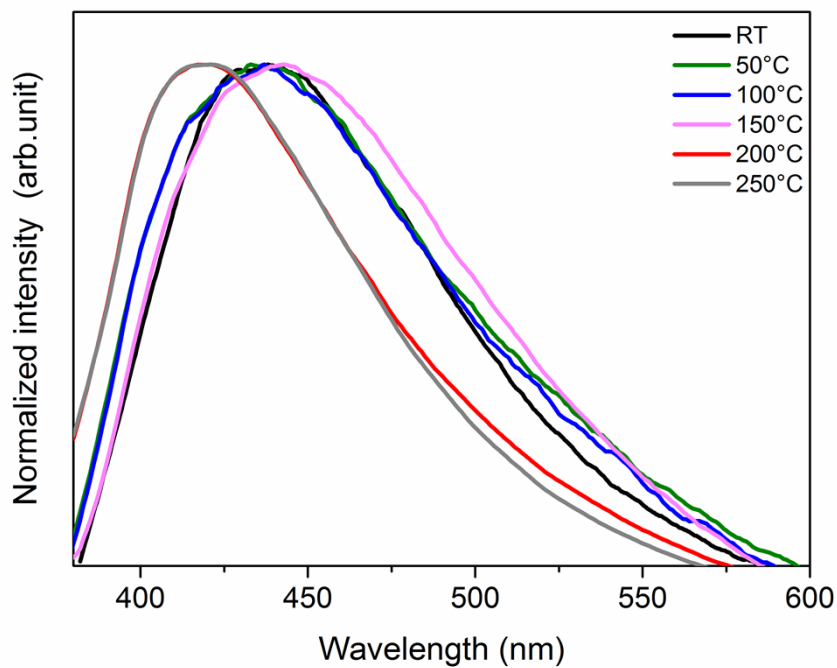


Fig. S12 Emission spectrum for Gd-IL ($\lambda_{em} = 350$ nm) with temperature variation.

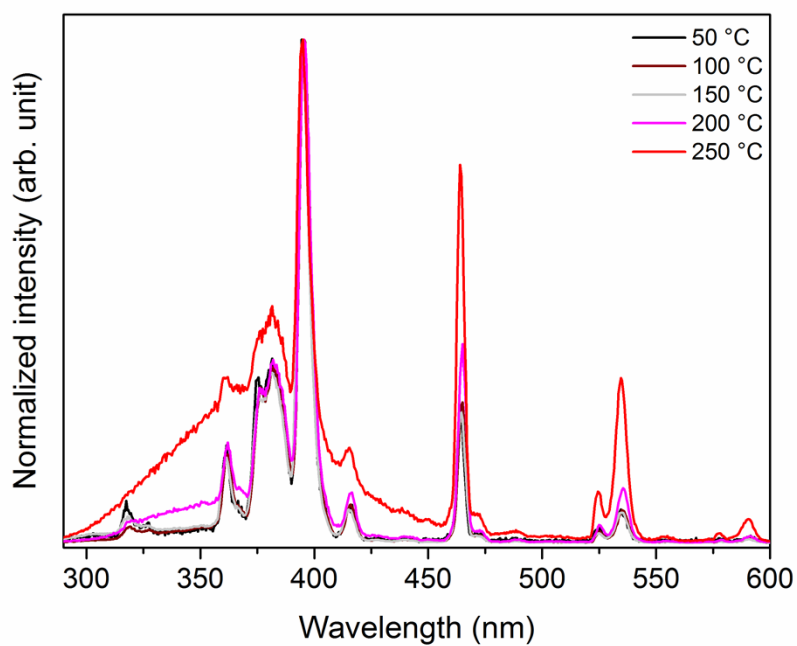


Fig. S13 Excitation spectrum for Eu-IL ($\lambda_{em} = 616$ nm) with temperature variation.

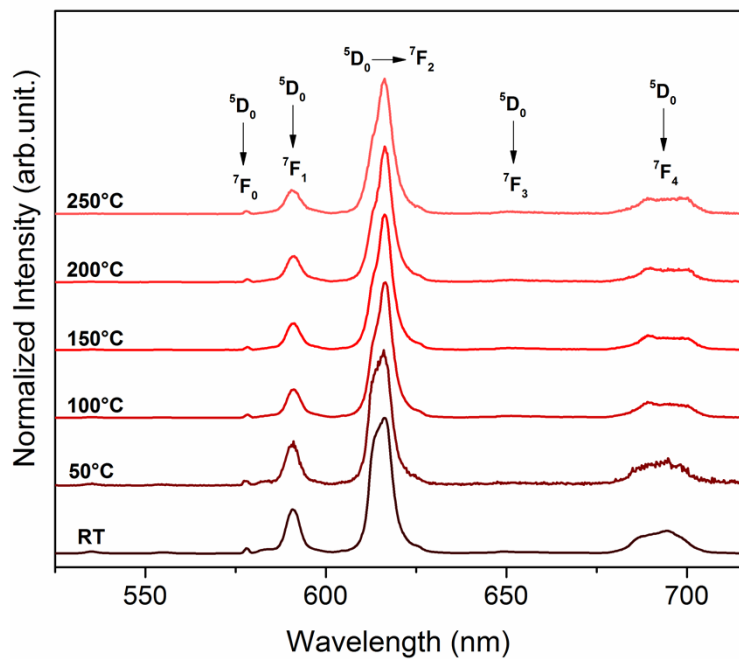


Fig. S14 Emission spectrum for Eu-IL ($\lambda_{\text{exc}} = 395$ nm) with temperature variation.

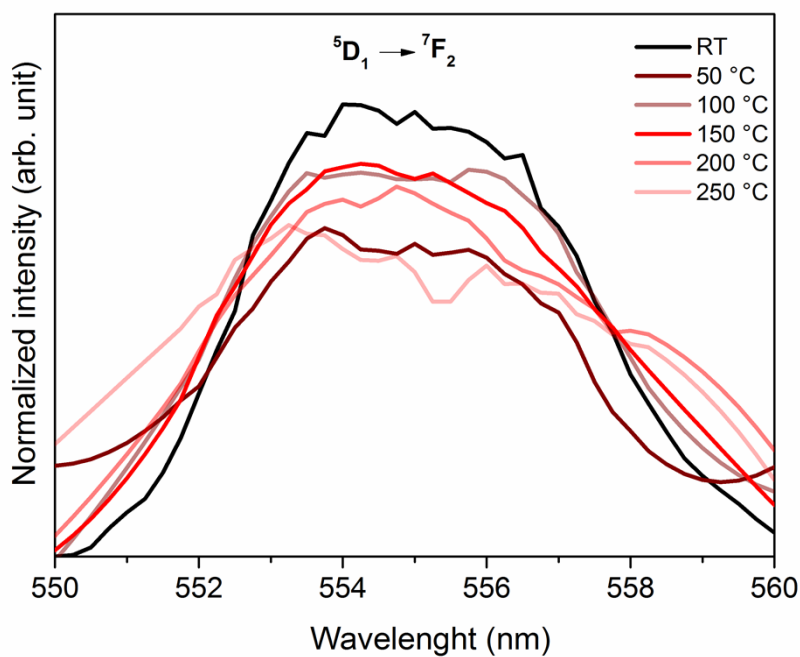


Fig. S15 ${}^5\text{D}_1 \rightarrow {}^7\text{F}_2$ transitions in the emission spectrum for Eu-IL ($\lambda_{\text{exc}} = 395$ nm) with temperature variation.

SUPPORTING INFORMATION

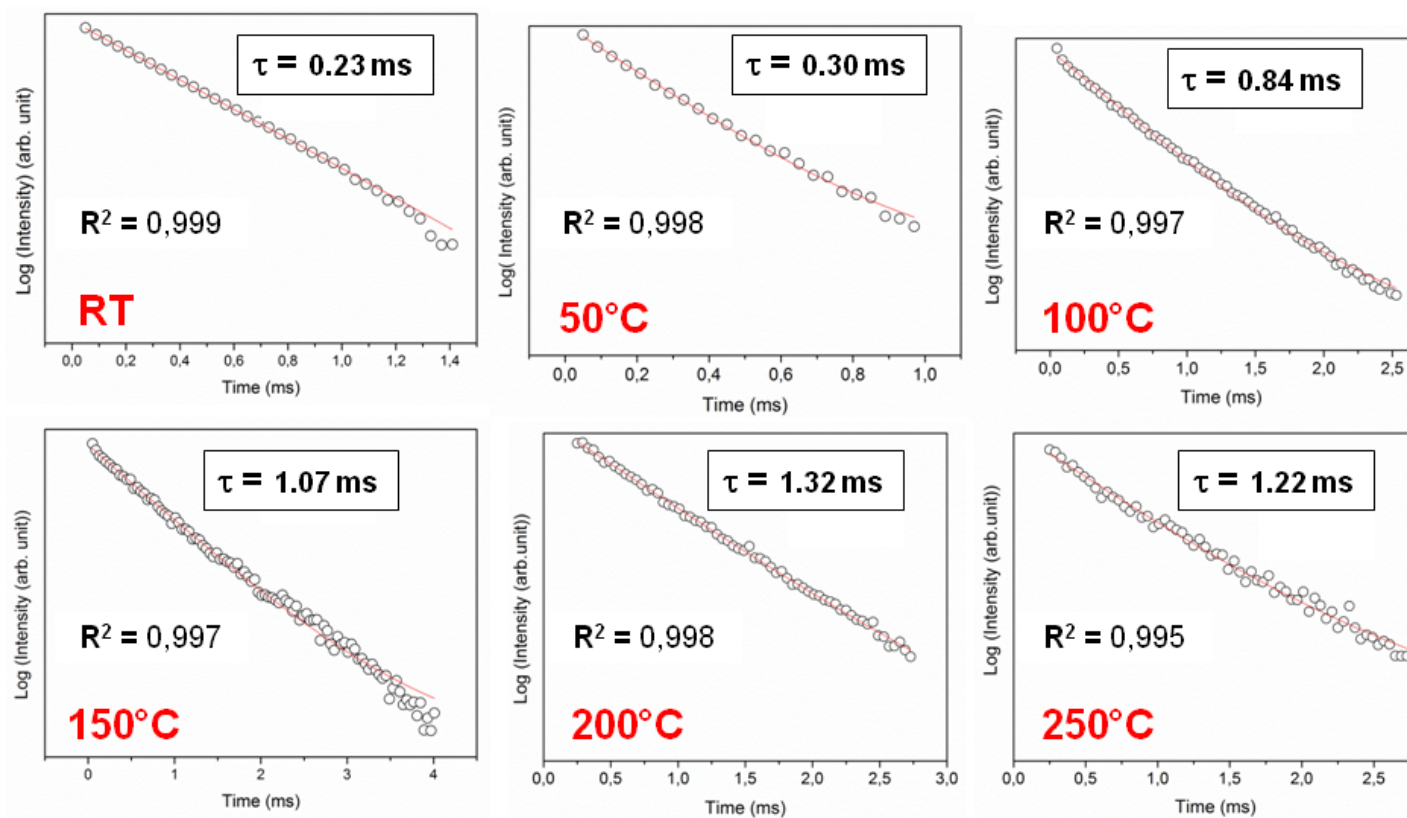


Fig. S16 Exponential decay curves for the Eu-IL in function of temperature variation.

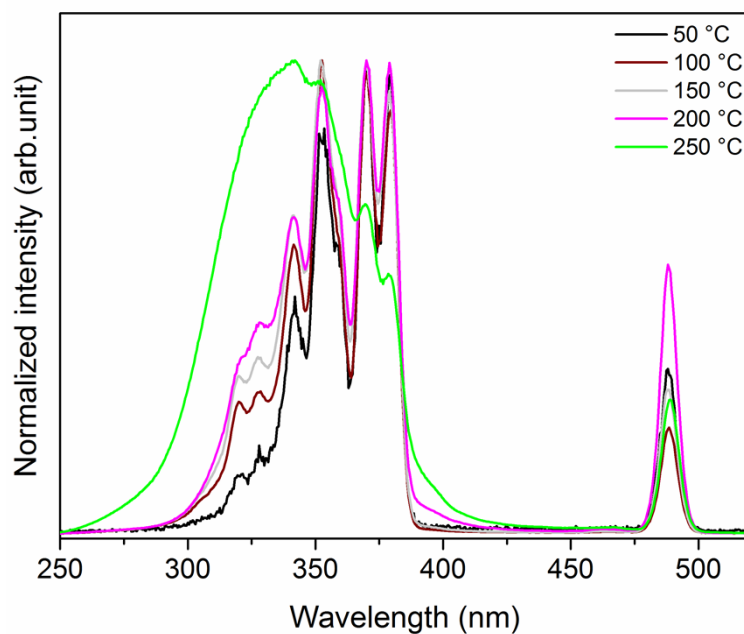


Fig. S17 Excitation spectrum for Tb-IL ($\lambda_{Em} = 542$ nm) with temperature variation.

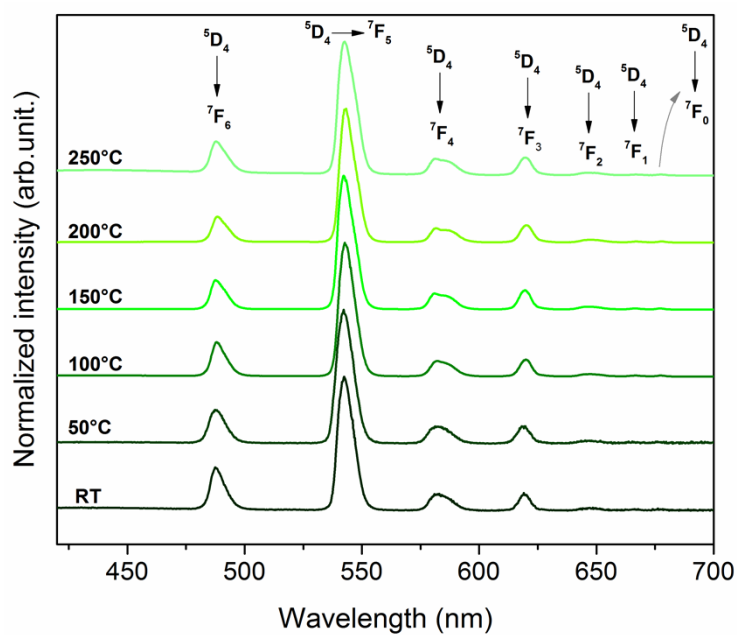


Fig. S18 Emission spectrum for Tb-IL ($\lambda_{exc} = 370$ nm) with temperature variation.

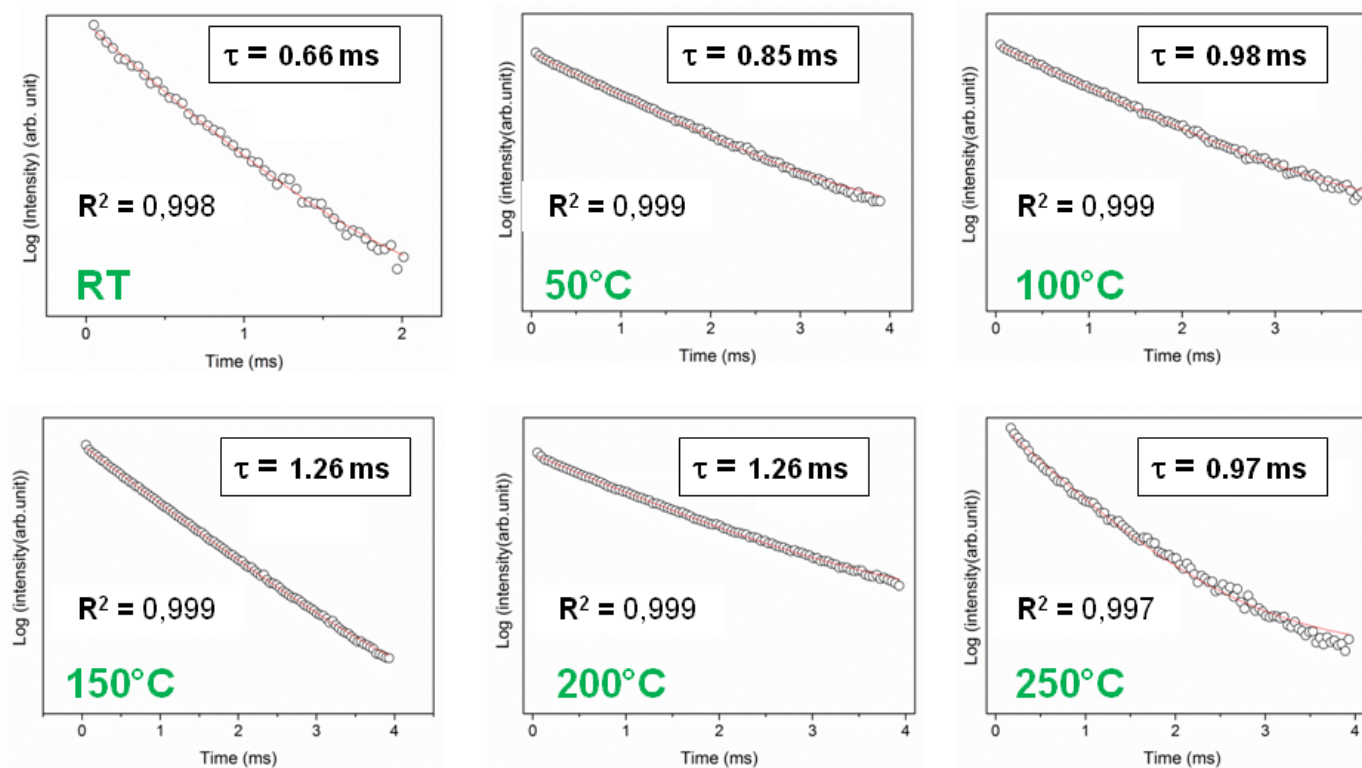


Fig. S19 Exponential decay curves for the Tb-IL in function of temperature variation.

SUPPORTING INFORMATION

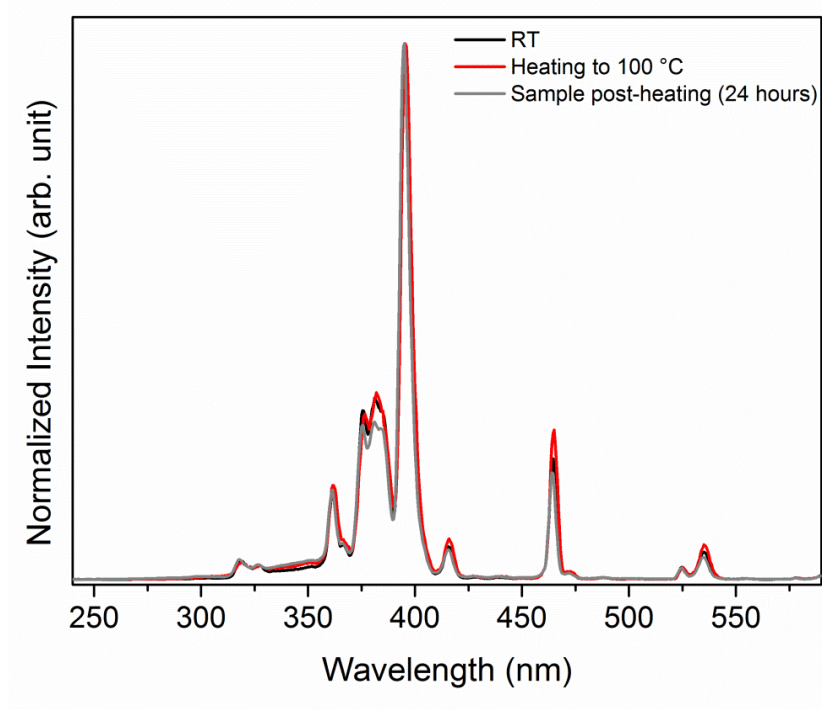


Fig.S20 Reversibility experiment for the excitation spectrum of Eu-IL. System at room temperature (black), under heating to 100 °C (red) and after 24 hours in contact with moisture (gray).

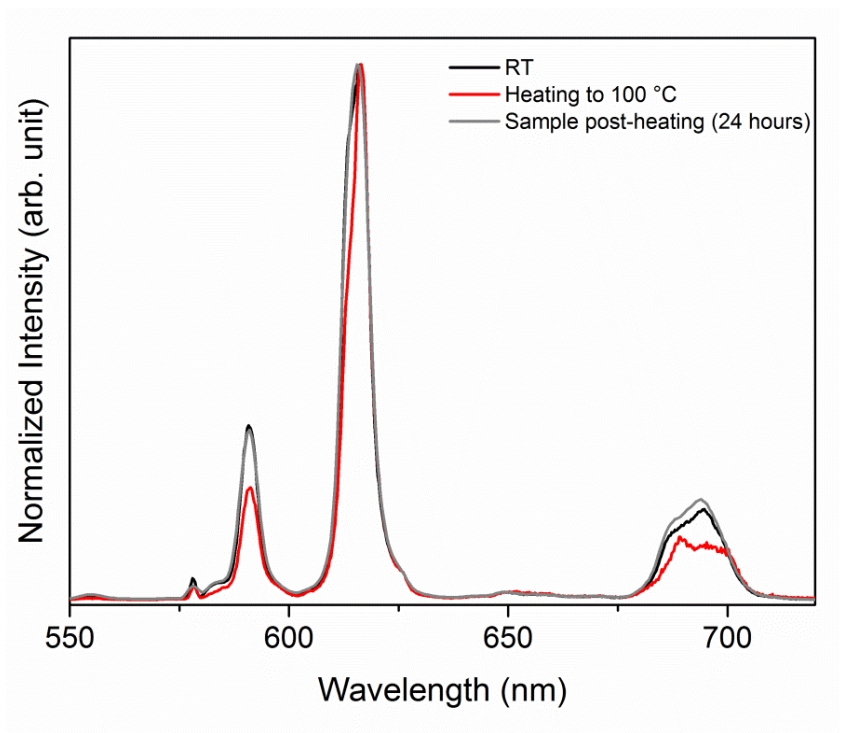


Fig. S21 Reversibility experiment for the emission spectrum of Eu-IL. System at room temperature (black), under heating to 100 °C (red) and after 24 hours in contact with moisture (gray).

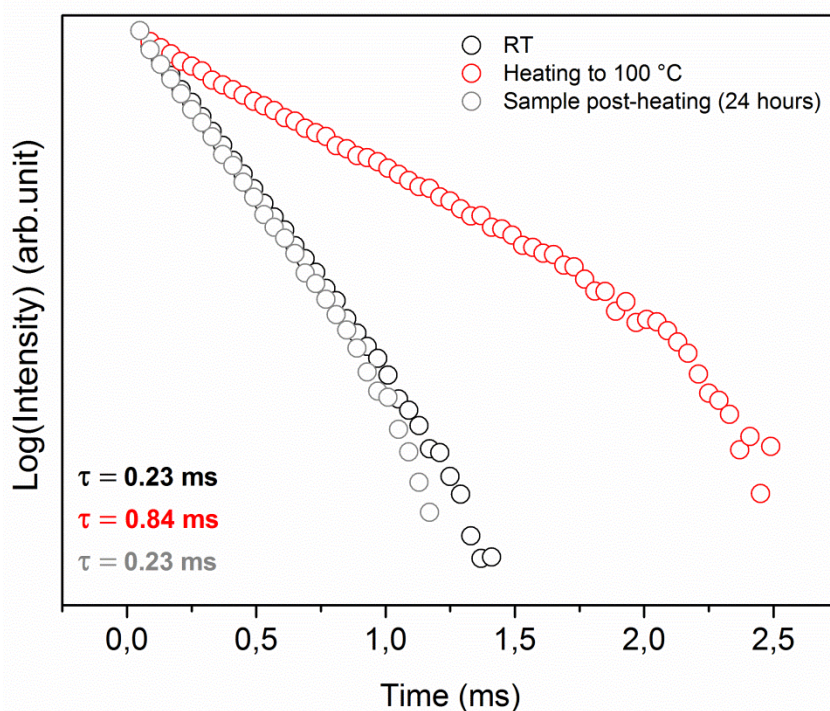


Fig.S22 Reversibility experiment for exponential decay curves of Eu-IL. System at room temperature (black), under heating to 100 °C (red) and after 24 hours in contact with moisture (gray).

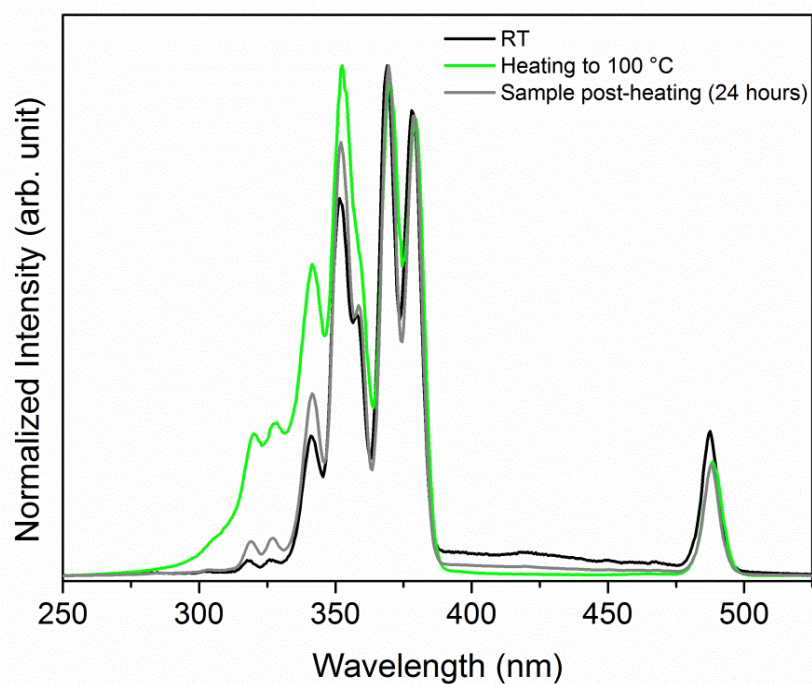


Fig.S23 Reversibility experiment for the excitation spectrum of Tb-IL. System at room temperature (black line), under heating to 100 °C (green) and after 24 hours in contact with moisture (gray).

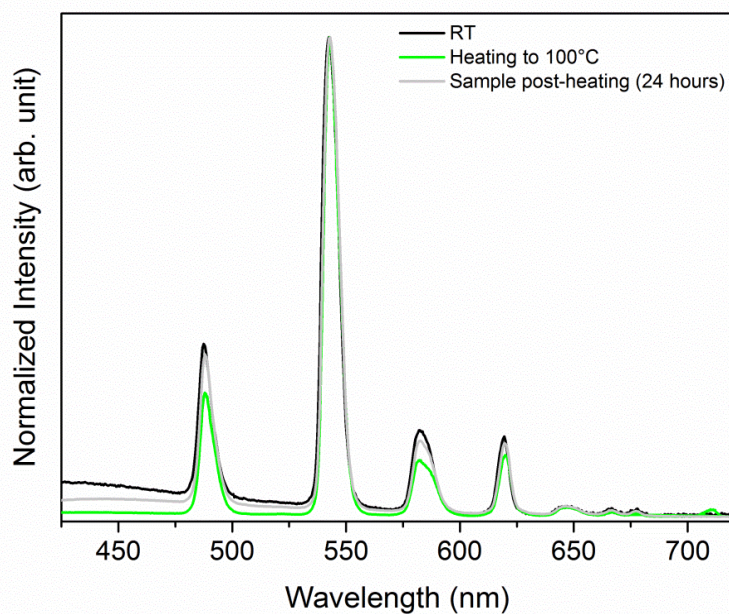


Fig.S24 Reversibility experiment for the emission spectrum of Tb-IL. System at room temperature (black), under heating to 100 °C (green) and after 24 hours in contact with moisture (gray).

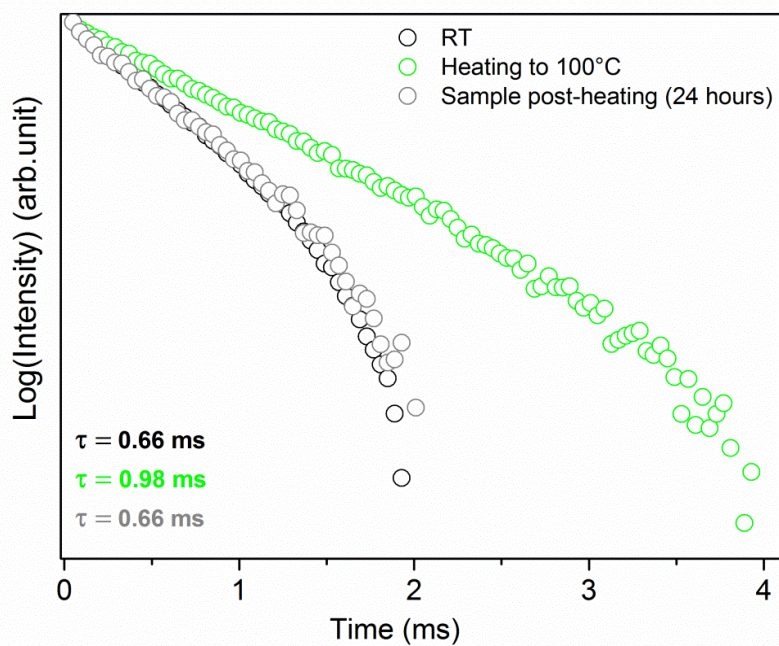


Fig.S25 Reversibility experiment for exponential decay curves of Tb-IL. System at room temperature (black), under heating to 100 °C (green) and after 24 hours in contact with moisture (gray).

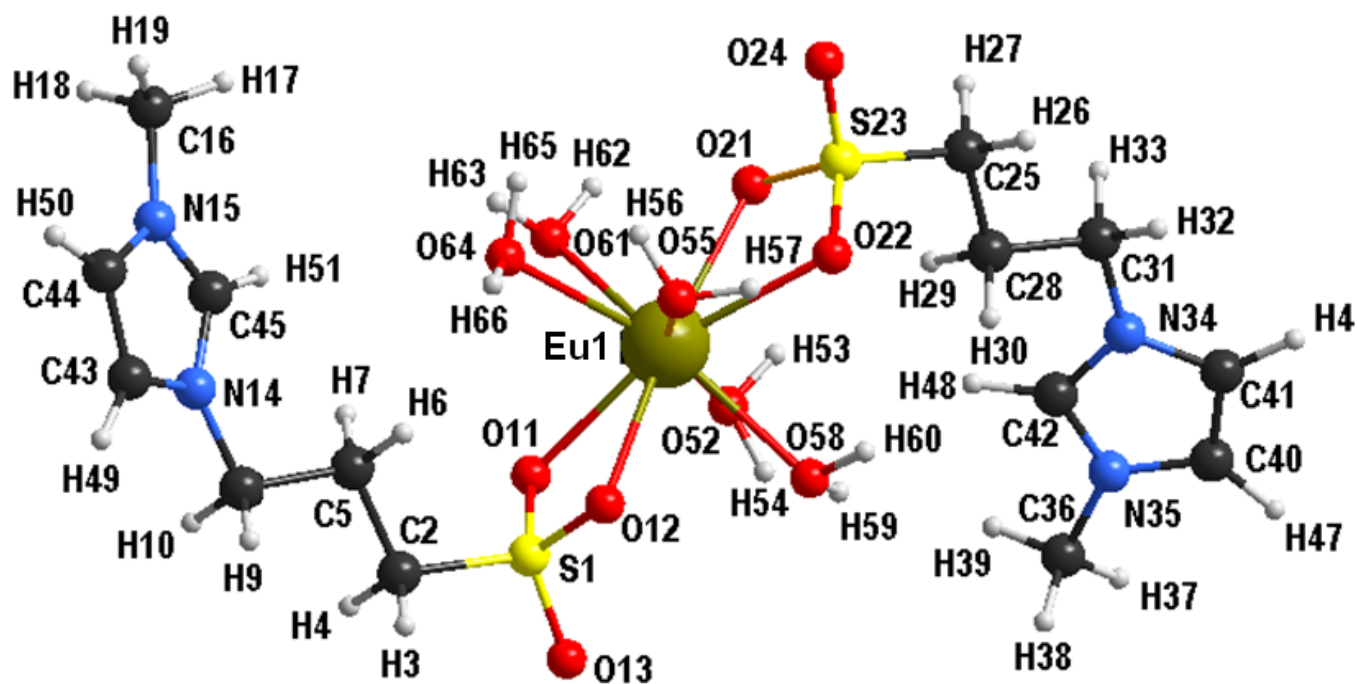


Fig. S26 Coordination environment formed by ionic liquids and metal center of Europium.

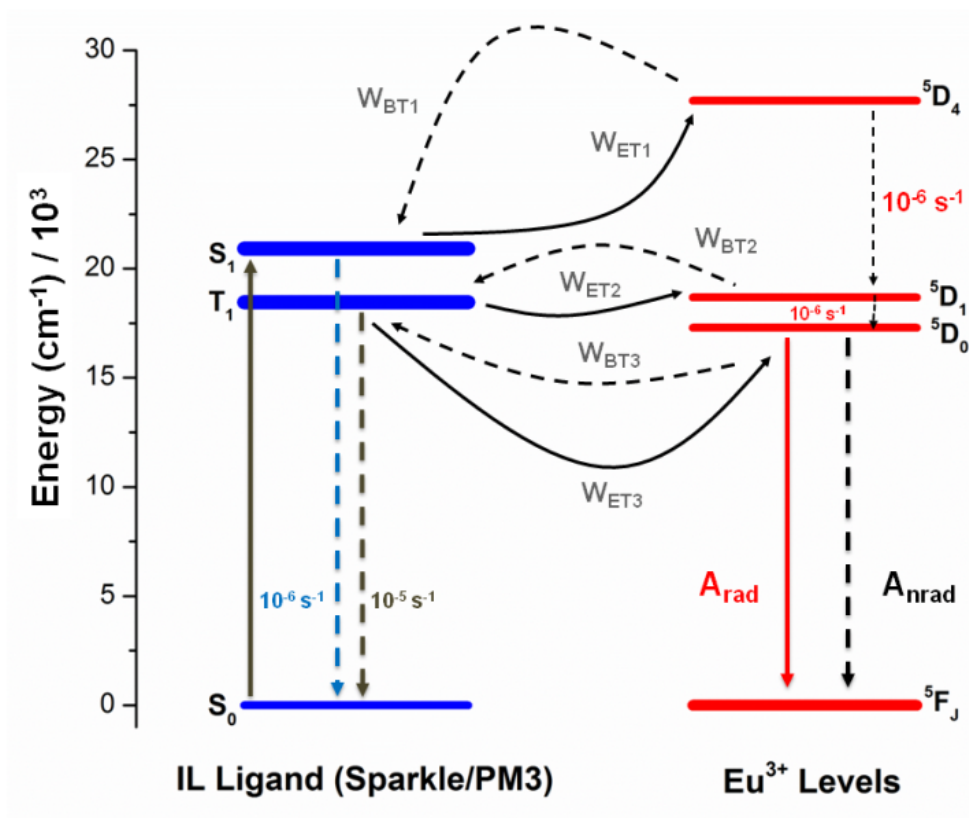


Fig. S27: Energy level diagram for Eu-IL complex, showing the most probable channel for intramolecular energy transfer.

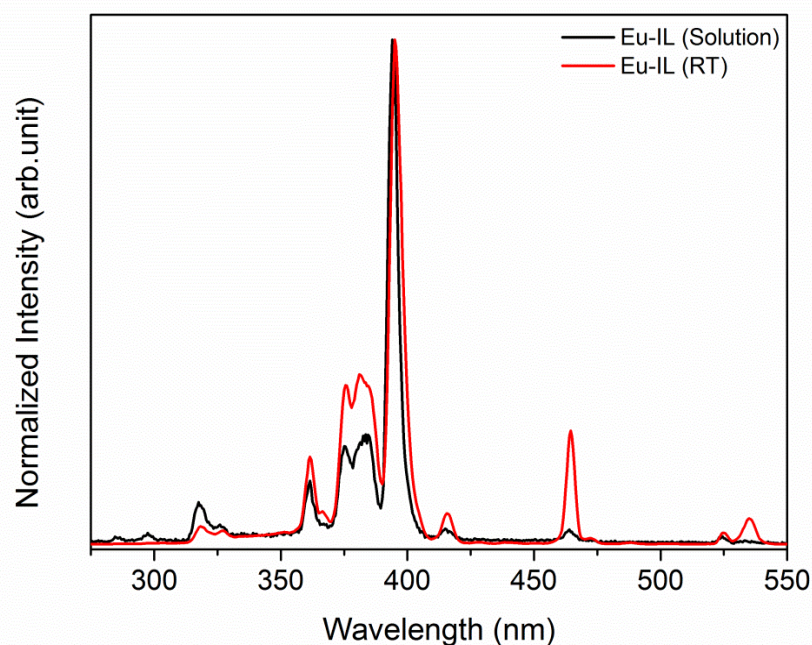


Fig. S28 Comparison of excitation spectrum for Eu-IL ($\lambda_{\text{em}} = 616 \text{ nm}$) obtained for the solution and RT conditions.

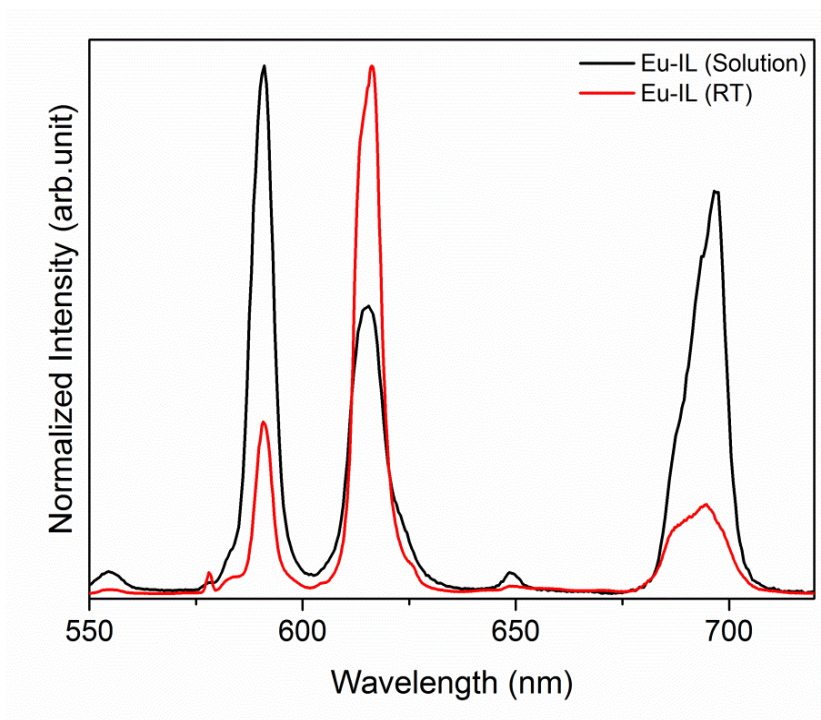


Fig. S29 Comparison of emission spectrum for Eu-IL ($\lambda_{\text{exc}} = 395$ nm) obtained for the solution and RT conditions.

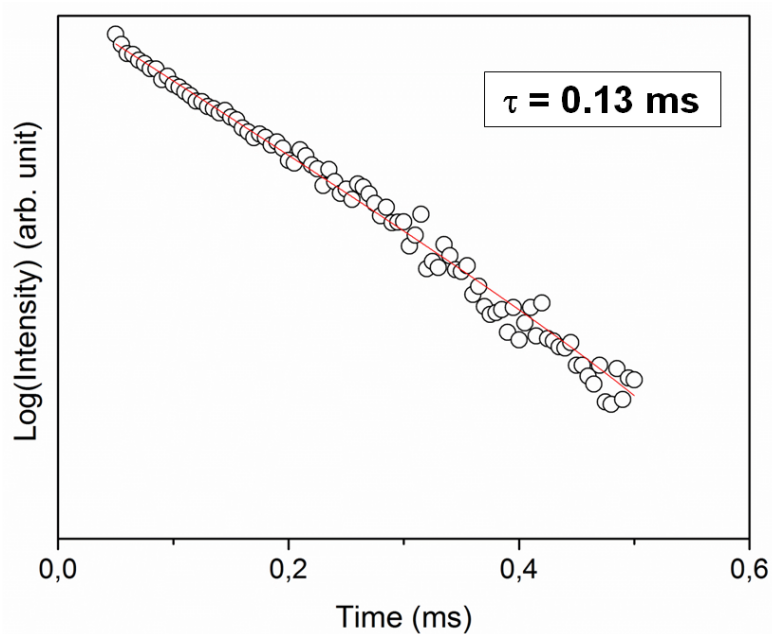


Fig. S30 Lifetime obtained for Eu-IL in solution ($\lambda_{\text{exc}} = 395$ nm and $\lambda_{\text{em}} = 616$ nm).

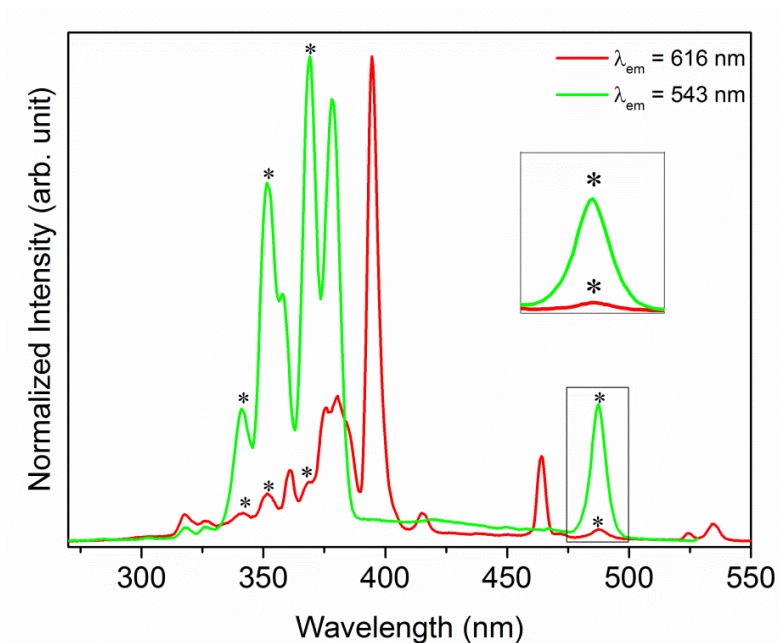


Fig. S31. Excitation spectrum of the mixed system $Tb_{25\%}Eu_{25\%}Gd_{50\%}$ -IL monitored at 616 nm (red line) compared with the spectrum of Tb-IL compound monitored at 543 nm (green line).

The FT-IR spectrum shown in Fig. S32 of the IL and mixed system. It's noted that absorption bands related in 3090 cm^{-1} , 1460 cm^{-1} , 1575 cm^{-1} and 1650 cm^{-1} are consistent for C-H bonds in imidazole ring^[1], CH_2 , and C=C and C=N^[2], respectively. This absorption bands are observed, in both materials, corresponding upkeep the structure of the ionic liquid after reaction. Even as bands in the range of 1575 cm^{-1} can be attributed to ring stretching of the imidazolium of the IL^[3]. The stretching symmetrical 1035 cm^{-1} and $1180/1300\text{ cm}^{-1}$ asymmetric, which can be applied to stretch S=O^[2] and appear shifted to lower energy regions in the mixed system. This indicates that the metal ion coordinating with the ionic liquid at this point. The region between $750\text{--}1000\text{ cm}^{-1}$ is consistent to S-O stretch and pronounced in IL and $Tb_{25\%}Eu_{25\%}Gd_{50\%}$ -IL. The broadband at 3500 cm^{-1} which corresponds to stretch O-H from water, and indicates an increase in the hydrophilic character of luminescent material in relation to IL. The result identified at approximately 3200 cm^{-1} N-H indicates the intermolecular hydrogen bond in the gel phase, as previously reported^[4].

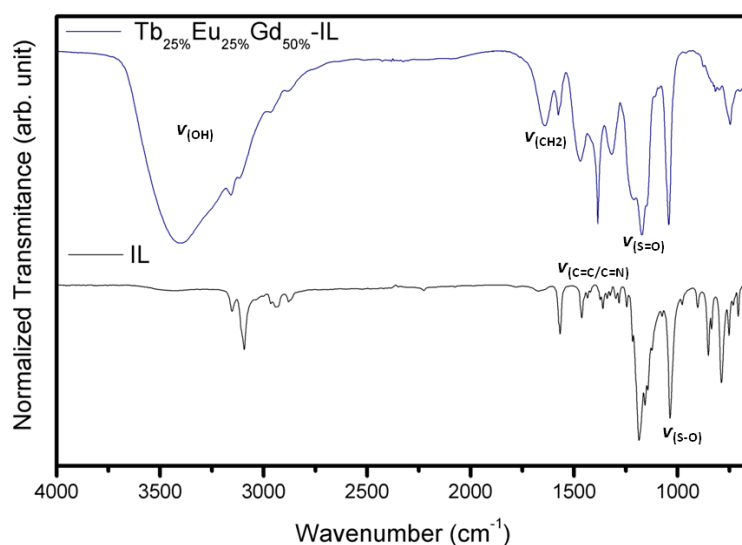


Fig. S32 Infrared spectrum for Ionic Liquid (IL) and mixed system ($Tb_{25\%}Eu_{25\%}Gd_{50\%}$ -IL).

In thermalgravimetric analysis to mixed system (Tb25%Eu25%Gd50%–IL) we see 4 events exactly as to isolated compounds Gd–IL, Tb–IL, and Eu–IL. To first event at approximately 106°C is related to moisture loss. The second event identified in 215°C show degradation to methyl and propane chain, follow to da removal of the NO₃⁻, approximately at 300°C, as first observed^[5]. The event found in ~380°C implies in degradation to imidazole ring. At last, was identified the thermal degradation for sulfonate group in 560°C.

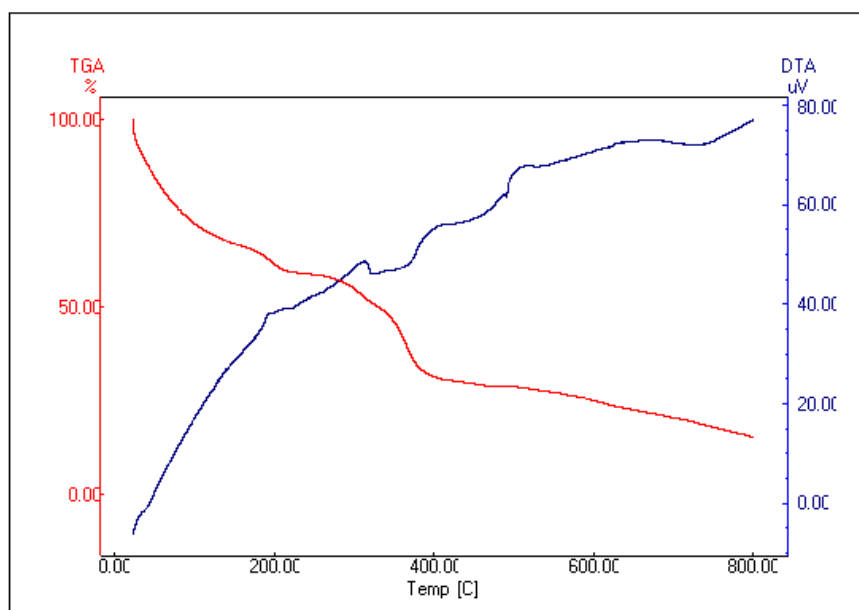


Fig. S33 Thermalgravimetric analysis to mixed system (Tb25%Eu25%Gd50%–IL)

1. Köckerling, T.P.a.M., *Imidazolium-Based Zwitterionic Butane-1-sulfonates: Synthesis and Properties of 4-(1-(2-Cyanoethyl)imidazolium)butane-1-sulfonate and Crystal Structures of 4-(1-Alkylimidazolium)butane-1-sulfonates (Alkyl = Methyl, Ethyl, Propyl)*. *Z. Anorg. Allg. Chem.*, 2011. **637**: p. 870–874.
2. Hua Li, J.L., Jiang Zhu, and Hongkai Wang, *Preparation of Novel Ionic Liquids and Their Applications in Brominating Reaction*. *Journal of the Korean Chemical Society*, 2011. **55**: p. 685-690.
3. Fan Zhou, T.W., Zhiqiang Li and Yige Wang, *Transparent and luminescent ionogels composed of Eu³⁺-coordinated ionic liquids and poly(methyl methacrylate)*. *Luminescence*, 2015.
4. Jong Hwa Jung, S.S., and Toshimi Shimizu, *Spectral Characterization of Self-Assemblies of Aldopyranoside Amphiphilic Gelators: What is the Essential Structural Difference between Simple Amphiphiles and Bolaamphiphiles?* *Chem. Eur. J.*, 2002. **8**: p. 2684-2690.
5. Stern, K.H., *High Temperature Properties and Decomposition of Inorganic Salts Part 3. Nitrates and Nitrites*. *J. Chem. Phys.*, 1972. **1**: p. 746-772.